Controlled Orientation of Cyclodextrin Derivatives Immobilized on Gold Surfaces

Gabriele Nelles, Michael Weisser, Roberta Back,* Peter Wohlfart, Gerhard Wenz,*,‡ and Silvia Mittler-Neher*

Contribution from the Max-Planck-Institut für Polymerforschung, Ackermannweg 10, 55128 Mainz, Germany

Received November 27, 1995[⊗]

Abstract: Several different cyclodextrinthiol derivatives have been immobilized on gold surfaces through a chemisorption process to form films which exhibit significantly different features. Three monothiolated cyclodextrin derivatives with different spacers between the cyclodextrin cavity and the thiol group and a mixture of multithiolated cyclodextrins were synthesized and characterized. Chemisorption of these compounds onto gold surfaces gave films which were investigated by Fourier transform infrared (FTIR) spectroscopy, time-of-flight mass spectrometry, contact angle measurements, plasmon surface polariton (PSP) spectroscopy, and cyclic voltammetry. It was found that the chemical structure of each cyclodextrin derivative had a strong influence on the molecular architecture in the resulting films, and in particular on the orientation of the cyclodextrin torus. Models were developed to describe the molecular arrangement in the films.

Introduction

Molecular host−guest systems have attracted enormous research interest in recent years. By careful selection of host and guest molecules, specific properties of the resulting inclusion compounds can be targeted. Cyclodextrins are cyclic oligosaccharides, the most commonly occurring of these consisting of six, seven, or eight glucopyranose units (α-, β- and γ-cyclodextrin, respectively).[1] The oligosaccharide ring forms a torus, with the primary hydroxyl groups of the glucose residues lying on the narrow side, and the secondary hydroxyl groups on the wider side. This structure, shown in Figure 1 for β-cyclodextrin, makes cyclodextrin a particularly versatile host molecule, with a great variety of possible guests, and it has already been employed in this capacity for a number of applications, including drug delivery control,[2] chromatography,[3] immobilization of chemically reactive materials,[4] solubility enhancement,[5] protection against photodegradation[6] or oxidation,[7] and selective removal of undesired substances.[8]

Many of the potential applications of host−guest systems require immobilization of either the host molecule or the guest molecule. Furthermore, host−guest interactions offer a novel approach to the stepwise functionalization of surfaces. Thus, a chemisorbed layer of host molecules offers a template upon which subsequent immobilization of guest molecules may occur. Supramolecular architectures, in which specific recognition

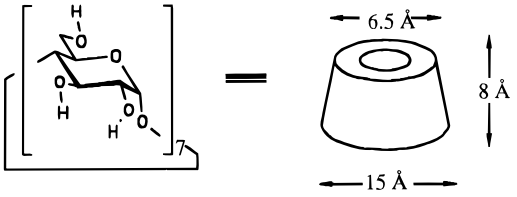

Figure 1. Structure and approximate dimensions of β-cyclodextrin. Note that, in subsequent figures, the cyclodextrin torus will be represented by the sketch shown here.

reactions are used to build upon intricate multilayered structure in a controlled fashion, are possible by this strategy.[9] For such systems, an exact knowledge of the molecular orientation within each layer is imperative, and control over this orientation is very advantageous.

Chung synthesized a 7-fold thiolated cyclodextrin and chemisorbed it onto gold and silver.[10] Electrochemical investigations indicated that relatively permeable films were formed, which is not surprising if one considers the lack of mobility the multithiolated cyclodextrins would have once they are adsorbed onto the gold surface. Permeability was observed to decrease in the presence of guest molecules.

Rojas et al.[11] synthesized a 7-fold thiolated β-cyclodextrin derivative and immobilized it on gold. However, again lateral diffusion of these derivatives, which would allow optimal packing within the adsorbed layer, would be negligible once immobilization has occurred (due to the multiple binding sites for each molecule), and the resulting coverages were submonolayer, typically 64−75%, as determined by reductive desorption of the thiol, with no apparent intermolecular organization. Maeda et al.[12] reported a 3-fold thiolated β-cyclodextrin derivative immobilized on colloidal silver which was examined

‡ Present address: Polymer Institut der Universität Karlsruhe, Hertzstrasse 16, 76187 Karlsruhe, Germany.

⊗ Abstract published in *Advance ACS Abstracts,* April 15, 1996.

(1) (a) Saenger W. *Angew. Chem., Int. Ed. Engl.* **1980**, *19*, 344. (b) Wenz G. *Angew. Chem., Int. Ed. Engl.* **1994**, *33*, 803.

(2) (a) Lach, J. L.; Chin, T.-F. *J. Pharm. Sci.* **1964**, *53*, 924. (b) Hassan, H. G.; Renck, H.; Lindberg, B.; Lindquist, H.; Aackerman, B. *Acta Anaestesiol. Scand.* **1985**, *29*, 380.

(3) Wiedenhof, N. *Stärke* **1969**, *21*, 63.

(4) Akito, E.; Nakajima, Y.; Horioka, M. *Jpn. Kokai* **1975**, *75* (129), 520.

(5) Schlenk, H.; Sand, D. M. *J. Am. Chem. Soc.* **1961**, *83*, 2312.

(6) Yamamoto, I.; Unaqi, T.; Suzuki, Y.; Katsuda, Y. *J. Pesticide Sci.* **1976**, *1*, 41.

(7) Szejtli, J.; Bolla-Pusztai, E.; Szabo, P.; Ferenczy, T. *Pharmacie* **1980**, *35*, 779.

(8) Kiji, J.; Konishi, H.; Okano, T.; Terashima, T.; Motomura, K. *Angew. Makromol. Chem.* **1992**, *199*, 207.

(9) Spinke, J.; Liley, M.; Guder, H.-J.; Angermaier, L.; Knoll, W. *Langmuir* **1993**, *9*, 1821.

(10) Chung, C. Ph.D. Thesis, Iowa State University, Ames, IA, 1990.

(11) Rojas, M. T.; Königer, R.; Stoddart, J. F.; Kaiffer, A. E. *J. Am. Chem. Soc.* **1995**, *117*, 336.

(12) Maeda, Y.; Kitano, H. *J. Phys. Chem.* **1995**, *99*, 487.

S0002-7863(95)03981-3 CCC: $12.00

by SERR spectroscopy. However, no quantitative analysis of coverage was given, and it would be expected that the multiple binding sites of each molecule would inhibit lateral diffusion, and hence high coverage. In the former work, coadsorption of *n*-pentanethiol with thiolated cyclodextrin was found to improve blocking of the gold surface to external redox species.

In this work the immobilization of several thiolated cyclodextrins on gold was investigated. In particular, the influences of the spacer length between the thiol group and the cyclodextrin cavity, and the number of thiol groups, on film structure were examined. Three monothiolated cyclodextrin derivatives with different spacer lengths between the cyclodextrin ring and the thiol group were synthesized and characterized. A mixture of multithiolated compounds was also prepared that each contain more than one thiolated spacer group on the primary side of the cyclodextrin ring (typically between two and four). All of these cyclodextrin derivatives were covalently bound to gold surfaces via chemisorption of the thiol groups to gold.[13] The structure of the resulting layers, the optical thickness, the packing density, the chemical composition, and the surface wettability were investigated by Fourier transform infrared (FTIR) spectroscopy,[14] time-of-flight mass spectrometry,[15] contact angle measurements,[16] plasmon surface polariton (PSP) spectroscopy,[17] and cyclic voltammetry.[18]

Experimental Section

Synthesis. NMR spectra were recorded with a Bruker AC 300 spectrometer (^{1}H, 300 MHz; ^{13}C, 75 MHz). Chemical shifts are reported in parts per million (ppm) downfield of TMS. Fast atom bombardment (FAB) mass spectra were recorded with a Fisons ZAB2-SE-FPD mass spectrometer with a cesium ion source and positive ion detection. FTIR spectra were recorded with a Bruker IFS 28 spectrometer. Samples were prepared as KBr pellets.

β-Cyclodextrin was dried overnight at 100 °C in vacuum prior to use. Pyridine and *N*,*N*-dimethylformamide (DMF) were freshly distilled from CaH_2. All other reagents were of the highest available commercial quality and used without further purification.

Mono(6-*O*-*p*-tolylsulfonyl)-β-cyclodextrin (1). Compound **1** was prepared as described in ref 19. The crude product was recrystallized twice in acetone (yield 2.5 g, 17.5%).

Mono[6-Deoxy-6-[(mercaptodecamethylene)thio]]-β-cyclodextrin (2) (CD(10)). Reaction of **1** with 1,10-decanedithiol in aqueous Na_2CO_3 containing 20% ethanol at 50 °C gave **CD(10)**. The crude product was purified on a reversed-phase column (RP-18) (yield 85.5 mg, 17%).

Mono[6-Deoxy-6-[[[(mercaptoethoxy)ethoxy]ethyl]thio]]-β-cyclodextrin (3) (CD(8)). Reaction of **1** with triethylene dithioglycol[20] in aqueous Na_2CO_3 containing 20% ethanol at 50 °C gave **CD(8)**. The crude product was purified on a reversed-phase column (RP-18) (yield 92 mg, 19.7%).

Mono(6-Deoxy-6-mercapto)-β-cyclodextrin (4) (CD(0)). Reaction of **1** with thiourea in DMF at 75 °C gave **CD(0)**. The crude product was recrystallized twice in acetone, and then freeze dried. The isothiouronium salt was then converted to the thiol with sodium disulfite ($Na_2S_2O_5$) (yield 72 mg, 27%).

Heptakis(6-*O*-*tert*-butyldimethylsilyl)-β-cyclodextrin (5). Compound **5** was prepared by reaction of *tert*-butyldimethylsilyl chloride with β-cyclodextrin in pyridine at 0 °C.

Heptakis[2,3-*O*-dimethyl-6-*O*-(*tert*-butyldimethylsilyl)]-β-cyclodextrin (6). Compound **6** was prepared by reaction of **5** with sodium hydride in DMF at 0 °C, and then methyl iodide in DMF at room temperature.

Heptakis(2,3-*O*-dimethyl)-β-cyclodextrin (7). Compound **7** was prepared by reaction of **6** and tetra-*n*-butylammonium fluoride solution (THF) in DMF at room temperature.

Heptakis(2,3-*O*-dimethyl)oligo(6-*O*-*p*-tolylsulfonyl)-β-cyclodextrin (8). Compound **8** was prepared by reaction of **7** with *p*-toluenesulfonyl chloride in pyridine at 0 °C. The crude product was purified by column chromatography.

Heptakis(2,3-*O*-dimethyl)oligo[6-deoxy-6-[(mercaptodecamethylene)thio]]-β-cyclodextrin (9) (CDx(10)). Reaction of **8** with 1,10-decanedithiol in a suspension of K_2CO_3 in DMF at 40 °C gave **CDx(10)**. The crude product was purified by column chromatography (yield 20 mg, 21% for 3-fold substitution).

Immobilization of Cyclodextrins on Gold. The cyclodextrin derivatives were chemisorbed on freshly evaporated gold films supported by Schott LaSFN9 glass substrates. All cyclodextrin adsorption solutions were 1×10^{-4} M in ethanol, and were centrifuged through a 0.2 μm filter (Millipore) to remove undissolved material. Typical adsorption times were 18−20 h, except for the surface plasmon spectroscopy experiments, which were performed after 30 min adsorption times.[21]

FTIR Studies. The adsorbed films were investigated by grazing incidence reflectance with a Perkin-Elmar ratio recording infrared spectrometer, model 1430. FTIR spectra of KBr pellets were recorded with a Bruker IFS 28 spectrometer.

Time-of-Flight Mass Spectrometry. The measurements were performed using a linear time-of-flight (TOF) mass spectrometer at a pressure of approximately 1×10^{-6} mbar. The cyclodextrin films were deposited on 50 nm gold films evaporated on glass slides that were first covered with a 2 nm chromium film in order to increase the mechanical stability of the gold film. Atomar and molecular ions from the sample were released by spontaneous desorption, a secondary ion process.[15b] Primary ions of adsorbates are field desorbed from the edges of an acceleration grid placed in front of the sample. These ions are accelerated toward the sample, gaining kiloelectronvolt energies. They finally sputter secondary ions from the sample, which are analyzed with the time-of-flight (TOF) mass spectrometer. Spectra of negative secondary ions are recorded using the simultaneously emitted secondary electrons from the sample surface as trigger particles. Acceleration voltages of 8.0−9.5 kV were applied to the sample. The recording time of a spectrum was 20−40 min. For each spectrum, the mass peaks of interest were integrated and normalized to the number of start events with one or more corresponding stop events. This leads to a relative ion yield that can be compared to the intensities of equivalent peaks in different spectra.

Contact Angle Measurements. Advancing and receding contact angles of water on the films were measured using a contact angle microscope (Krüss G-1) under ambient conditions, while the volume of the drop (2.5 μL) was increased or decreased at the minimum rate required for movement of the water/air/solid triple point.

Plasmon Surface Polariton Spectroscopy. A diagram of the plasmon surface polariton spectroscopy setup is shown in Figure 2. A modified Kretschmann configuration is used[22] with a 50 nm gold film evaporated onto a glass substrate, which is then optically matched to the base of a 90° LaSFN9 glass prism ($n = 1.85$ at $\lambda = 632.8$ nm)

(13) (a) Dubois, L. P.; Nuzzo, R. G. *Annu. Rev. Phys. Chem.* **1992**, *43*, 437. (b) Grunze, M. *Phys. Scr.* **1993**, *T49*, 711.

(14) Arndt, T. Ph.D. Thesis, University of Mainz, Germany 1988.

(15) (a) Price, D.; Milnes, G. J. *Int. J. Mass Spectrom. Ion Processes* **1990**, *99*, 1. (b) Voit, H.; Schoppmann,C.; Brandl, D. *Phys. Rev. B* **1993**, *48*, 17517.

(16) Whitesides, G. M.; Laibinis, P. E. *Langmuir* **1990**, *6*, 87.

(17) Knoll, W. *MRS Bull.* **1991**, *7*, 29.

(18) Greef, R.; Peat, P.; Peter, L. M.; Plecher, D.; Robinson, J. *Instrumental Methods in Electrochemistry*; Ellis Horwood Series in Physical Chemistry; Ellis Horwood Limited, John Wiley & Sons: Chichester, 1985.

(19) (a) Melton, L. D.; Slessor, K. N. *Carbohydr. Res.* **1971**, *18*, 29. (b) Takahashi, K.; Hattori, K.; Toda, F. *Tetrahedron Lett.* **1984**, *25*, 3331. (c) Lincoln, S. F.; Coates, J. H.; Easton, C. J.; van Eyk, S. J.; May, B. M.; Singh, P.; Stile, M. A.; Williams, M. L. *Chem. Abstr.* **1991**, *114*, 88647; Patent Nr. WO/9002141, Australian Commercial Research and Development Ltd.

(20) Gift from E. Klemm, Institut für Organische Chemie und Makromolekulare Chemie, University of Jena.

(21) The film thicknesses, as measured by surface plasmon spectroscopy, were observed to reach their final value in the first 30 min. The permeabilities and densities of the films, as measured by the other characterization techniques, required much longer adsorption times before reaching stable values. Further kinetic investigations will be reported elsewhere: Weisser, M.; Nelles, G.; Wohlfart, P.; Wenz, G.; Mittler-Neher, S. Manuscript in preparation.

(22) Kretschmann, E. *Z. Phys.* **1971**, *241*, 313.

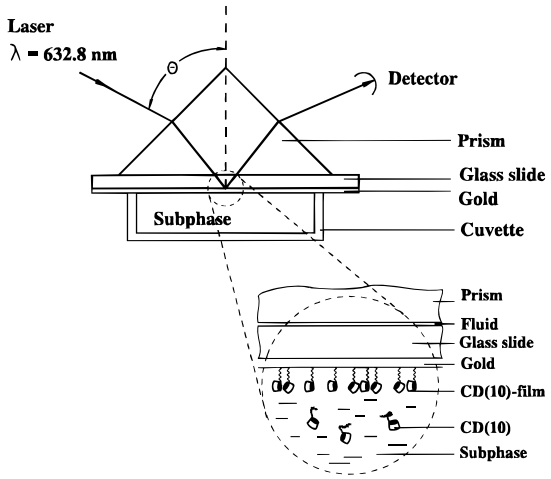

Figure 2. Schematic diagram of the experimental setup used for polariton surface plasmon characterization of film formation.

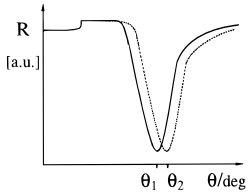

Figure 3. Schematic plasma surface polariton spectroscopy reflectivity curves without and with a chemisorbed dielectric layer on the gold film, with reflectance minima θ_1 and θ_2, respectively.

using an index matching fluid. The plasmon surface polaritons are excited at the metal/dielectric interface, upon total internal reflection of the laser beam (HeNe, $\lambda = 632.8$ nm, power 5 mW) at the prism base. By varying the angles of incidence of the laser beam, a plot of reflected intensity as a function of the angle of incidence is obtained, similar to that shown in Figure 3. The gold film is then exposed to a solution of the chemisorbing thiols in a cuvette, and the reflection curve shifts as chemisorption occurs, as a function of the optical thickness of the resulting film.

Cyclic Voltammetry. Cyclic voltammetry was performed using the evaporated gold films as the working electrodes. Specifically, a 2.4 × 1.4 cm^2 gold working electrode (evaporated onto LaSFN9 substrates using a mask), Ag/AgCl reference electrode (Bio Analytical Systems Inc.), and platinum wire auxiliary electrode were used. The cyclic voltammograms were measured in 0.1 M phosphate buffer (pH 7.4), 0.001 M $K_3[Fe(CN)_6]$, at a sweep rate of 100 mV/s, using a Princeton Applied Research 270 potentiostat.

Results

(A) Synthesis. The synthesis of the cyclodextrinthiols is shown schematically in Figure 4. Monofunctionalization (Figure 4a) of native cyclodextrin was achieved by introduction of a tosylate group, following the procedure of Melton and Slessor.[19a] The principal product under these conditions has one primary hydroxyl group per cyclodextrin molecule tosylated. After two recrystallization steps, pure mono(6-*O*-*p*-tolylsulfonyl)-β-cyclodextrin (**1**) was obtained. Although the yield, typically between 15% and 20%, was slightly lower than that obtained by Melton and Slessor, gram quantities could be obtained using this recrystallization process for purification, as opposed to column chromatography, which yields only subgram quantities.

Nucleophilic substitution with 1,10-decanedithiols or triethylene dithioglycol[20] lead to mono[6-deoxy-6-[(mercaptodecamethylene)thio]]-β-cyclodextrin (**CD(10)**) (**2**) or mono[(6-deoxy-6-[[[(mercaptoethoxy)ethoxy]ethyl]thio]]-β-cyclodextrin (**CD(8)**) (**3**), respectively.[23] Mono(6-deoxy-6-mercapto)β-cyclodextrin (**CD(0)**) (**4**) was obtained through reaction of thiourea with **1** to give the isothiouronium salt of cyclodextrin, which was then cleaved with disulfite to give the thiol.[24] A side product that appeared predominantly in basic solution was the mono(3,6-anhydro)β-cyclodextrin.[25] This compound has the same R_f value, but is more water soluble than native β-cyclodextrin.

Multitosylation (Figure 4b) of native β-cyclodextrin occurs at both the primary and secondary hydroxy groups, and it is difficult to separate the resulting products. For this reason, when multitosylation is desired only at the primary hydroxyl groups, it is necessary to first block the secondary hydroxyl groups. In order to do this, the primary hydroxyl groups were protected by silylation with *tert*-butyldimethylsilyl chloride (**5**).[26,27] Following this, the secondary hydroxyl groups were methylated to give **6**,[27,28] and then the *tert*-butyldimethylsilyl groups were removed from the primary hydroxyls.[28,29] The resulting heptakis(2,3-*O*-dimethyl)-β-cyclodextrin (**7**) could then be tosylated by the same procedure as was used for the monofunctionalization, but with excess *p*-toluenesulfonate.[30] The resulting cyclodextrin tosylates **8** were found to have between two and four tosylate substituents. Reaction with 1,10-decanedithiol led to the multithiolated heptakis(2,3-*O*-dimethyl)oligo[6-deoxy-6-[(mercaptodecamethylene)thio]]-β-cyclodextrin (**CDx(10)**) (**9**). It was not possible to separate the different multithiolated species in this mixture further by column chromatography, as each species has several isomers itself, leading to broad elution bands for the 2-fold, 3-fold, and 4-fold substitutes which overlap with one another.

All intermediates and end products were characterized by ^{1}H NMR, ^{13}C NMR, and mass spectrometry. FTIR spectroscopy was also used for additional characterization.

(B) Evidence for Immobilization of Cyclodextrin on Gold Surfaces. In order to determine the success of immobilizing these cyclodextrin derivatives on gold, FTIR spectroscopy and time-of-flight mass spectrometry were employed. FTIR spectra of bulk samples (as KBr pellets) and of the chemisorbed films were recorded and compared in order to verify the presence of cyclodextrin derivatives on the gold substrates. The time-of-flight mass spectrometry was used to identify the characteristic molecular fragments of the cyclodextrin derivatives on gold.

(1) FTIR Spectroscopy. Representative FTIR spectra of bulk (upper) and film (lower) samples are shown in Figure 5 for **CD(0)** (Figure 5a) and **CD(10)** (Figure 5b). For both derivatives, the characteristic vibrations of cyclodextrin can be identified in both the bulk and film spectra.[31] The three most intense bands between 1155 and 1030 cm^{-1} correspond to the

(23) Hirotsu, K.; Higuchi, T. *J. Org. Chem.* **1982**, *47*, 1143.
(24) (a) Fujita, K.; Ueda, T.; Imoto, T.; Tabushi, I.; Toh, N.; Koga, T. *Bioorg. Chem.* **1982**, *11*, 72. (b) Kubik, S; Wulff, G. *Macromol. Chem. Phys.* **1994**, *195*, 1719.
(25) The per(3,6-dianhydro)-β-cyclodextrin has already been described: (a) Gadelle, A; Defaye, J. *Angew. Chem.* **1991**, *103*, 94. (b) Ashton, P. R.; Ellwood, P.; Station, I.; Stoddart, J. F. *Angew. Chem.* **1991**, *103*, 96.
(26) (a) Fügedi, P. *Carbohydr. Res.* **1989**, *192*, 366. (b) Collaboration with A. Stein, Institut für Organische Chemie und Makromolekulare Chemie, University of Jena. (c) Icheln, D. Ph.D. Thesis, Institut for Organische Chemie, University of Hamburg, Germany, 1993.
(27) (a) Takeo, K.; Mitoh, H.; Uemura, K. *Carbohydr. Res.* **1989**, *187*, 203. (b) Takeo, K.; Uemura, K., Mitoh, H. *J. Carbohydr. Chem.* **1988**, *7*, 293.
(28) Personal communication from D. Icheln and B. Gehrcke, Institut für Organische Chemie, University of Hamburg, and A. Stein, Institut für Organische Chemie und Makromolekulare Chemie, University of Jena.
(29) Corey, E. J.; Venkateswarlu, A. *J. Am. Chem. Soc.* **1972**, *94*, 6190.
(30) Yi, G.; Bradshow, J. S.; Rossiter, B. E.; Malik, A.; Li, W.; Lee, M. L. *J. Org. Chem.* **1993**, *58*, 4844.
(31) (a) Casu, B.; Reggiani, M. *Tetrahedron* **1968**, *24*, 803. (b) Russel, N. R.; McNamara, M. *J. Inclusion Phenom. Mol. Recognit. Chem.* **1989**, *7*, 455.

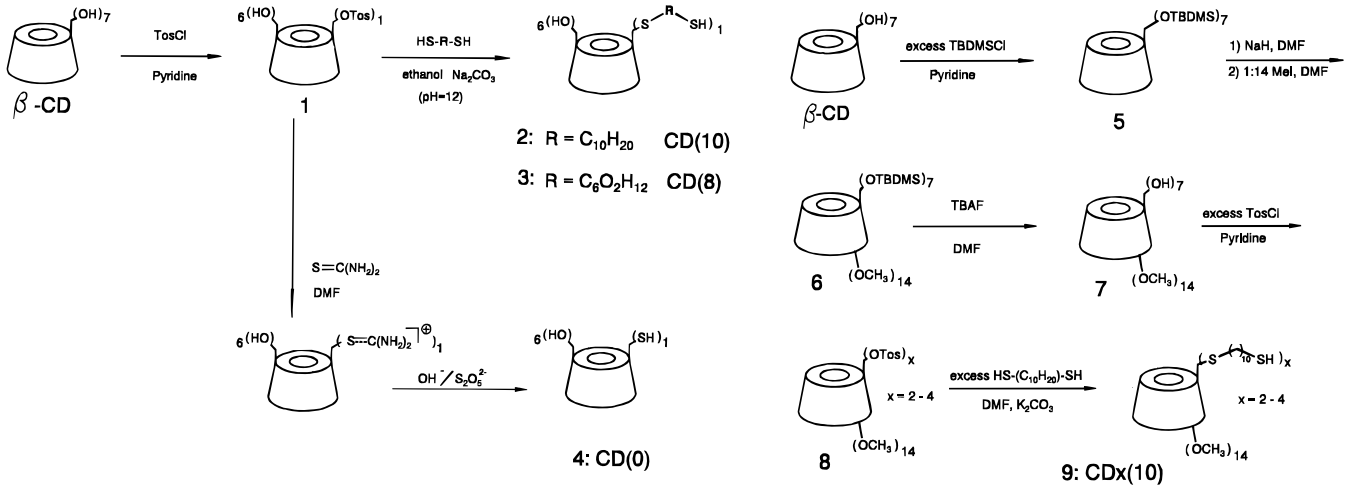

Figure 4. Synthetic scheme: (a, left) monofunctionalization, (b, right) multifunctionalization.

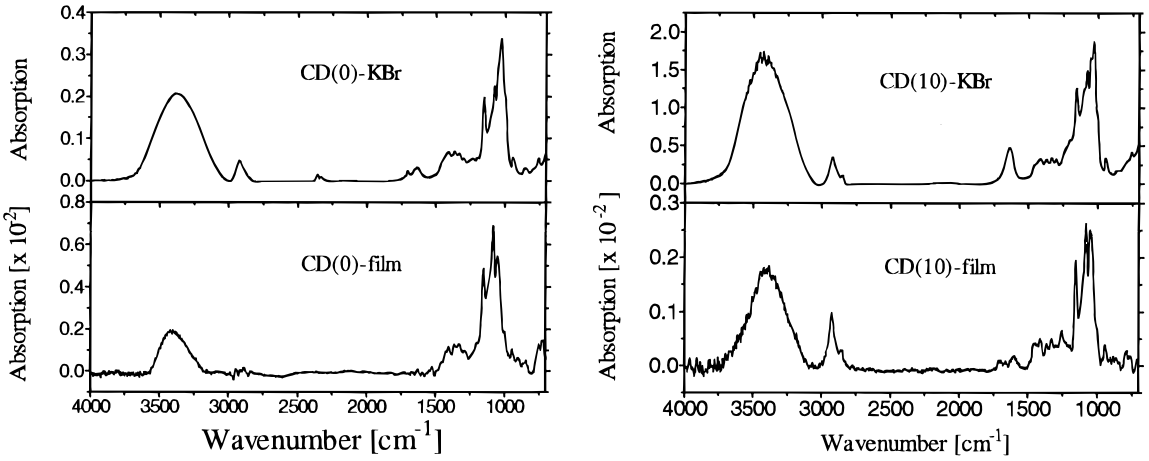

Figure 5. FTIR spectrum for bulk (upper) and film (lower) samples: (a, left) **CD(0)**, (b, right) **CD(10)**.

antisymmetric glycosidic ν_a(C−O−C) vibrations, and the coupled ν(C−C/C−O) stretch vibration. The deformation vibrations δ(C−H) and δ(O−H) of the CH_2 and OH groups between 1460 and 1299 cm^{-1} and the characteristic ring vibrations at 945 and 705 cm^{-1} are seen in all spectra, thus providing strong evidence for the presence of the cyclodextrin derivatives at the gold surface.

The peak assignments for the various C−H, C−O, and C−C vibrations could not be determined, owing in part to the difficulty in determining the dipole moment of the cyclodextrin ring, and in part to the added complication of the spacer units in the derivatized cyclodextrin. However, qualitative orientational information could be extracted from a comparison of the bulk and film spectra, specifically with respect to peak shifts and intensity changes, as the film spectra contain only those vibrations with a dipole moment component perpendicular to the gold surface.

For all cyclodextrin derivatives, the ν_a(C−O−C) vibration appears in the KBr spectrum and in the film spectrum at almost the same wavenumber. The relative intensities of the ν(C−C/C−O) stretch vibrations differ in the bulk and film spectra. In the bulk spectra the band at 1030 cm^{-1} is the most intense, whereas in the film spectra the band at 1084 cm^{-1} is the most intense.

In the KBr spectra the antisymmetric vibrational bands of the CH_2 groups are found at 2927 cm^{-1} (**CD(0)**) and at 2924 cm^{-1} (**CD(10)**). In the **CD(10)** spectrum the symmetric C−H vibration is also visible at 2853 cm^{-1}. The ν_a(C−H) vibrational band for **CD(0)** in the film spectrum is very weak relative to the bulk spectrum. In contrast, the spectrum of the immobilized **CD(10)** shows the ν_a(C−H) vibrational band shifted to 2927 cm^{-1} and its relative intensity with respect to the coupled ν(C−C/C−O) vibrational band increased. The intensity of the symmetric ν_s(C−H) vibrational band at 2852 cm^{-1} is also increased relative to the coupled ν(C−C/C−O) vibration band.

The O−H vibrational band is broadened in all spectra, bulk and film, presumably due to inter- and intramolecular hydrogen bonding. Furthermore, by comparing the frequency of the O−H vibrational bands in the KBr spectra and the film spectra, one finds a small bathochromic shift in the **CD(10)** film and a small hypsochromic shift in the **CD(0)** film.

(2) Time-of-Flight Mass Spectrometry. To investigate the chemical composition of a monolayer on a molecular level, mass analysis is very useful. In the time-of-flight mass spectrometry experiment, the sample surface is bombarded with kiloelectronvolt ions, and atoms and molecules are released to the gas phase, partially as ions. Negatively charged secondary ions are analyzed with a linear time-of-flight mass spectrometer. A bare gold substrate and gold substrates covered with chemisorbed cyclodextrins were investigated. Typical mass spectra of negative ions from a bare gold surface and a **CD(10)** film on gold are shown in Figure 6. In the spectrum of the bare gold surface (Figure 6a) the dominant peaks correspond to Au^- ions, Au_n^- ions, and ions of gold combined with surface contaminants. The **CD(10)** spectrum also shows the Au^- peak, but with much lower intensity. In the spectrum of the **CD(10)** film (Figure 6b), the dominant peaks originate from fragments of the **CD(10)** molecules. Such substance-specific peaks were

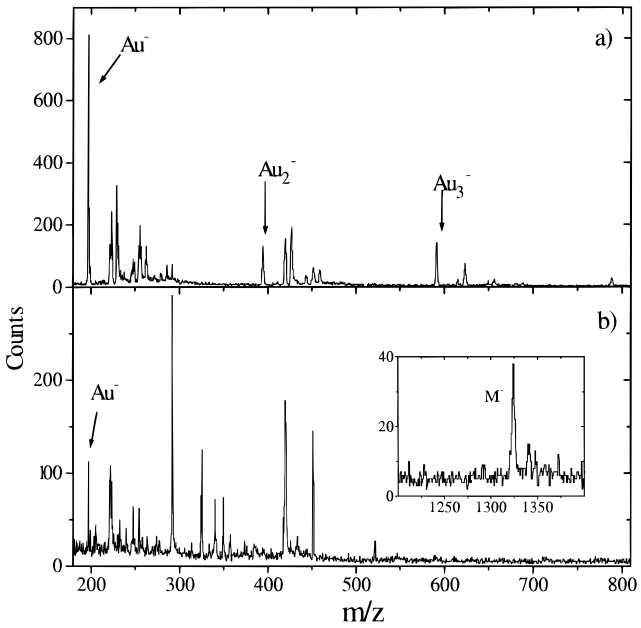

Figure 6. Spontaneous desorption mass spectra of negative ions from (a) a bare gold substrate and (b) a chemisorbed film of **CD(10)** on gold. M^- represents the deprotonated molecular ion.

Table 1. Advancing and Receding Contact Angles and the Hysteresis of these, for Chemisorbed Films of **CDx(10)**, **CD(0)**, **CD(8)**, **CD(10)**, and Octadecanethiol

	CDx(10)	**CD(0)**	**CD(8)**	**CD(10)**	$C_{18}H_{37}SH$
advancing contact angle	50 ± 3	31 ± 2	30 ± 2	26 ± 2	111 ± 1
receding contact angle	18 ± 3	6 ± 3	8 ± 3	12 ± 2	100 ± 1
hysteresis of contact angle	32 ± 3	25 ± 3	22 ± 3	14 ± 2	10 ± 1

detected in all chemisorbed cyclodextrin films examined. In particular, the deprotonated molecular ions M^- can be observed in all films of monothiolated derivatives. For the multithiolated derivatives, only the fragment with one decanethiol group could be detected. This is attributed to the low probability of desorption for derivatives with more than one thiol "anchor".

(C) Molecular Architecture in Immobilized Films. To gain more precise insight into the molecular architecture of the films, several complementary techniques were employed. Contact angle measurements gave information on the air/film interface, plasmon surface polariton spectroscopy measured optical thicknesses of films, and cyclic voltammetry gave information about film permeabilities.

(1) Contact Angle Measurements. Contact angles of water on a surface can be a measure of the hydrophilicity or hydrophobicity of that surface. Small angles usually indicate a hydrophilic surface, whereas large angles indicate a hydrophobic surface. Results from the measurement of advancing and receding contact angles are listed in Table 1. For comparison, the well-characterized system of self-assembled octadecanethiol monolayers[32] has been measured, and the data are included in Table 1. The contact angles show a hydrophilic surface for the cyclodextrin monothiolated derivatives, whereas the alkanethiol gives a hydrophobic surface. The film of the multithiolated cyclodextrin mixture gives a slightly higher contact angle than the monothiolated species, indicating increased hydrophobicity, as expected from the methylation on the secondary side of the cyclodextrin ring. The hysteresis of the contact angles, a measure for the surface roughness, is strongly correlated to the spacer length for the monothiolated derivatives, with the **CD(10)** film exhibiting the least hysteresis of all the cyclodextrin derivatives. The multithiolated mixture shows a larger hysteresis than all the other cyclodextrin derivatives.

Table 2. Theoretical Thickness and Experimental Thickness Calculated from Plasmon Surface Polariton Spectroscopic Data Assuming a Refractive Index of 1.5 for the Organic Films

	CDx(10)	**CD(0)**	**CD(8)**	**CD(10)**	$C_{18}H_{37}SH$
theoretical thickness (nm)	2.3	1.3	2.5	2.9	2.2
experimental thickness (nm)[a]	2.1	1.0	2.1	2.5	2.0

[a] ± 0.2

(2) Plasmon Surface Polariton Spectroscopy. The results from the surface plasmon measurements are given in Table 2 together with theoretical film thicknesses. The theoretical film thicknesses were calculated using the known dimensions of the β-cyclodextrin torus[1] and a C−C bond distance of 0.15 nm. In this calculation, molecular models were constructed in which all of the molecules have fully extended alkyl chains. The cyclodextrin ring in the models of the monothiolated compounds is tilted to give the longest possible dimensions for each derivative, and in the model of the multithiolated compounds it is taken to have the C_n axis perpendicular to the surface normal. The results presented in Table 2 are based on reflected intensity versus incident angle plots such as that shown in Figure 3. The reflected intensity shows a sharp minimum at the resonance angle, (θ_1 for bare gold), which depends upon the precise architecture of the metal/dielectric interface and is defined by the matching condition for energy and momentum between the evanescent photons and the plasmon surface polaritons. From a Fresnel fit to the resonance curve for bare gold surfaces, it is possible to obtain the product of the dielectric function and the thickness of the gold layer. Addition of a thin layer to the surface of the gold typically shifts the position of the resonance to higher angles (θ_2), and fitting this second curve gives the optical thickness of the layer. Although surface plasmon measurements allow the determination of an average optical thickness of an adsorbed film, accurate conversion of this optical thickness to a geometrical thickness requires knowledge of the refractive index of the film, a parameter which depends on both the molecular composition of the film and its packing density. In practice, it is not possible to distinguish between a thin film with a high refractive index and a film twice as thick but with half the contrast in the medium. The present data are evaluated using a homogeneous refractive index of 1.5 for all cyclodextrin derivatives,[33] although it is expected that the cyclodextrin cavities will have a different dielectric constant than the spacers.

(3) Cyclic Voltammetry. In a usual cyclic voltammetry investigation of a reversible redox pair at an unmodified electrode surface, the redox currents are proportional to the electrode area. Thus, for modified electrode surfaces with decreased electrode area available for redox processes, the redox currents are expected to decrease. Furthermore, as these redox currents are confined to smaller and smaller electrode areas, the current density increases, and regular Nernstian redox behavior is no longer observed. Therefore, cyclic voltammetry can be a useful probe of films immobilized on an electrode surface, and has already been used very effectively in the

(32) Hesse, M. *Spectroskopische Methoden in der organischen Chemie;* Georg Thieme Verlag: Stuttgart, 1987.

(33) Ulman, A. *An Introduction to Ultrathin Organic Films*; Academic Press, Inc.: New York, 1991.

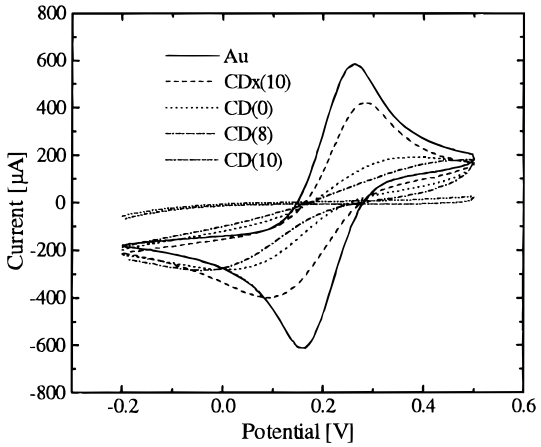

Figure 7. Cyclic voltammograms in 0.001 M $K_3[Fe(CN)_6]$/0.1 M phosphate buffer, pH 7.4, of a bare gold electrode and gold electrodes modified with chemisorbed films of **CD(0)**, **CD(8)**, **CD(10)**, and **CDx(10)**. All potentials are vs the Ag/AgCl reference electrode.

Table 3. Data from Cyclic Voltammograms Shown in Figure 7[a]

	gold	**CDx(10)**	**CD(0)**	**CD(8)**	**CD(10)**
$i_p^o(\mu A)$	669	500	160	100	10
$i_p^o(CD)/i_p^o(Au)$	1	0.75	0.24	0.15	0.015
ΔE_p (mV)	98	185	353	469	*b*
i_p^o/i_p^r	1.0	1.4	1.2	1.4	*b*

[a] i_p^o is the oxidative peak current, $i_p^o(CD)/i_p^o(Au)$ is the ratio of oxidative peak currents of cyclodextrin-modified gold to bare gold, ΔE_p is the separation between the oxidation and reduction peak potentials, and i_p^o/i_p^r is the ratio of oxidative to reductive peak currents. [b] Not measurable, due to a lack of the reductive peak.

investigation of several modified electrode systems, including alkanethiol films immobilized on gold.[34]

In this work, cyclic voltammetry was used as a qualitative tool to probe the density or permeability of cyclodextrin films on a gold electrode. The oxidation and the reduction processes of ferricyanide at the modified gold surfaces were investigated with respect to the molecular structure of the immobilized species, and compared to the same redox processes at a bare gold surface.

Cyclic voltammograms of $K_3[Fe(CN)_6]$ are shown in Figure 7 for gold working electrodes modified with the various cyclodextrin derivatives. The data are presented in Table 3. For all the films, the oxidation peak current, i_p^o, is lower than that for bare gold, and the peak potential separation, ΔE_p, is larger than that observed for bare gold. Furthermore, the ratio of oxidative to reductive peak currents, i_p^o/i_p^r, deviates from 1 for all films. These effects are observed to increase with increasing spacer length for the monothiolated cyclodextrins. The multithiolated derivatives showed the highest redox currents of all films, but also unusually large i_p^o/i_p^r values.

Discussion

Monothiolated cyclodextrin derivatives immobilized at a gold surface are reported here for the first time. In addition, a mixture of multithiolated cyclodextrin derivatives were synthesized and immobilized at gold surfaces for comparative purposes. Evidence for the successful immobilization of these compounds on gold was obtained from FTIR spectroscopy and time-of-flight mass spectrometry of the resulting films. In all of these chemisorbed films, the cyclodextrin cavities are believed to form the outermost layer of the system, as supported by the contact angle results, but it is possible to control the orientation of the cyclodextrin cavity by varying the number of thiol anchors and the length of spacer between the cavity and the thiol group. Each of the techniques used to characterize the films gave information on the orientation of these molecules in the films, leading to the proposal of a model describing the different molecular architectures believed to arise from the different cyclodextrin derivatives.

In the FTIR results, various changes in band intensities and positions from the bulk spectra to the film spectra suggest a different degree of order among the cyclodextrins in the bulk and film samples, imposed in the latter by the immobilization to the gold surface. In particular, the antisymmetric vibrational bands of the CH_2 groups in **CD(0)** are very weak in the film spectrum compared to the bulk. Since the C−H vibrations for **CD(0)** arise solely from the CH_2 groups on the glucose units in the cyclodextrin ring, this decreased intensity of the antisymmetric vibrational bands could indicate preferential alignment in the **CD(0)** film of these CH_2 groups parallel to the gold surface.[35] This in turn suggests that in the **CD(0)** film, the C_n axis of the torus is aligned preferentially perpendicular to the gold surface, as the dipole moments of these CH_2 groups lie perpendicular to the C_n axis of the torus. These data must be interpreted with caution, however, as the three negative peaks between 2800 and 3000 cm^{-1} indicate the presence of impurities in the reference spectrum, which was subtracted from the film spectrum. These impurities are inherent in the measurement method, and impossible to eliminate entirely, so it is not possible to rule out a small ν_a(C−H) vibrational band, obscured by the reference spectrum.

The increase of the C−H vibrational bands in the **CD(10)** film spectrum relative to the bulk spectrum suggests that some CH_2 groups are preferentially oriented perpendicular to the gold surface in the film sample. However, in **CD(10)**, the C−H vibrations arise from CH_2 groups both in the spacer and in the ring, and thus it is difficult when analyzing this increased intensity of C−H vibrations in the film spectrum to differentiate between alignment of the cyclodextrin ring and alignment of the spacer.

The broadened O−H vibrational band, indicating increased hydrogen bonding, may be further interpreted with regards to the observed frequency shift, as a shift to lower frequencies is known to occur when hydrogen bonding increases.[36] Such a shift is observed in the **CD(10)** film spectrum, and may be due to the long alkyl spacer in the **CD(10)** molecule, which could allow better packing of the immobilized rings, and hence possible optimization of intermolecular hydrogen bonding, unlike between **CD(0)** molecules, which are held too rigidly in place for this to occur. By the same interpretation, it can be concluded from the film spectra of **CD(8)** and **CDx(10)** that the former has strong intermolecular hydrogen bonding, optimized due to the mobility afforded by the triethylene glycol spacer, whereas the latter has only weak intermolecular hydrogen bonding, because of the mobility restrictions imposed by the multiple thiol anchors.

The mass spectra may also be used to probe the molecular architecture of the films. Specifically, the spectra from the cyclodextrin films show the Au^- peak observed for bare gold, but with attenuated intensity. This can be explained as a result of two effects of the chemisorbed films, one being the shielding of the gold from incoming primary ions and the other being

(34) (a) Porter, M. D.; Bright, T. B.; Allara, D. L.; Chidsey, C. E. D. *J. Am. Chem. Soc.* **1987**, *109*, 3559. (b) Finklea, H. O.; Avery, S.; Lynch, M.; Furtsch, T. *Langmuir* **1987**, *3*, 409. (c) Sabatini, E.; Rubenstein, I.; Maoz, R.; Sagiv, J. *J. Electroanal. Chem.* **1987**, *219*, 365.

(35) Dluhy, R. A. *J. Phys. Chem.* **1986**, *90*, 1373.

(36) Bain, C. D.;Troughton, E. B.; Tao, Y.-T.; Evall, J.; Whitesides, G. M.; Nuzzo, R. G. *J. Am. Chem. Soc.* **1989**, *111*, 321.

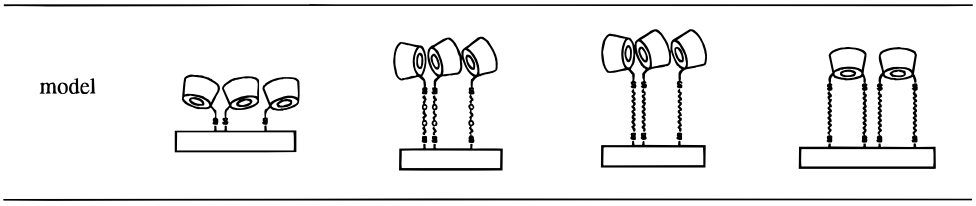

Figure 8. Models for the structure of the chemisorbed cyclodextrin films.

Table 4. Yield (Y) of Au^- and Au_2^- Ions of a Bare Gold Substrate and Chemisorbed Films of **CDx(10)**, **CD(0)**, **CD(8)**, and **CD(10)** on Gold[a]

	gold	**CDx(10)**	**CD(0)**	**CD(8)**	**CD(10)**
$Y(Au^-)$ ($\times 10^{-3}$)	12 ± 3	10 ± 1	4.8 ± 0.8	3 ± 1	2.3 ± 0.8
$Y(Au_2^-)$ ($\times 10^{-3}$)	2.8 ± 0.8	2.2 ± 0.2	0.7 ± 0.1	0.4 ± 0.2	0.3 ± 0.1
$f(Au^-)$	1	1.2 ± 0.3	2.5 ± 0.8	4 ± 0.5	5 ± 2
$f(Au_2^-)$	1	1.3 ± 0.3	4 ± 1	7 ± 2	9 ± 4

[a] These yields are expressed in desorption events of the particular gold ion, normalized to the total number of desorption events. $f(Au^-)$ is the screening factor for desorption of Au^- ions ($n = 1, 2$) and is defined as the following ratio: $Y(Au^-)$gold/$Y(Au^-)$thiol

the blocking of desorbed Au^- ions released from the gold. Both effects are determined by the permeability of the films. Thus, by comparing the yields of Au^- and Au_2^- ions from different cyclodextrin films, one can compare the packing density of these films. In Table 4 the yields of Au^- and Au_2^- ions from the films of different thiolated cyclodextrin derivatives are compared to the corresponding yields of Au^- and Au_2^- from the bare gold surface. The screening factor f is defined as the ratio of the Au_n^- yield from bare gold to the Au_n^- yield from cyclodextrin-modified gold, and describes the ability of the film to shield the gold layer against incoming primary ions as well as to block the release of desorbed gold ions. In this context, the screening abilities of chemisorbed cyclodextrin derivatives increase significantly with increasing spacer length. This is in agreement with the idea that improved packing is afforded by longer spacers for the monothiolated derivatives, as suggested by the FTIR spectroscopy results regarding intermolecular hydrogen bonding. For the multithiolated cyclodextrin mixture, poorer screening compared to all the monothiolated cyclodextrins was observed, again consistent with the FTIR spectroscopy results showing only weak hydrogen bonding in the **CDx(10)** films, presumably due to poor packing of these molecules on the gold surface.

Further support for this interpretation comes from the hysteresis data in the contact angle results, which indicate that **CD(10)** forms the most homogeneous surface of all the cyclodextrin derivatives, and the multithiolated cyclodextrin the least.

The thicknesses of the chemisorbed layers of all three monofunctionalized cyclodextrin derivatives as calculated from PSP spectroscopy data correlate well with the theoretically calculated thicknesses, suggesting a fully extended spacer chain. Presumably the experimentally determined thicknesses for all three films deviate slightly from the theoretically calculated thicknesses because the dielectric constant used in the fitting procedure is that of a closely packed organic monolayer, and the cyclodextrin films are believed to be loosely packed. The multithiolated derivative **CDx(10)** has an optical thickness less than the optical thickness of **CD(10)** which has the same length of spacer group. This result supports the proposed molecular orientation of **CDx(10)**, with the torus axis oriented normal to the sample surface.

The electrochemical results, including lower i_p^o values and larger ΔE_p values for all cyclodextrin derivatives relative to bare gold, indicate decreased electrode surface accessible to the redox species and increased current density on this available electrode surface. The **CD(10)** film formed the least permeable barrier of all the monothiolated cyclodextrin derivatives, again presumably due to the freedom of the cyclodextrin ring to orient at the end of the long spacer to optimize intermolecular interactions. This interpretation is supported by the fact that the **CD(0)** film provided the most permeable film of all the monothiolated derivatives, as the rings have little chance to orient and pack themselves effectively. The films of multithiolated cyclodextrins show the highest redox currents of all the cyclodextrin derivatives, indicating the highest permeability, but the i_p^o/i_p^r ratio is the highest of all cyclodextrin derivatives, indicating some irreversibility of the ferri/ferrocyanide redox couple. This still requires further investigation, and could be related to the relative accessibility of the cyclodextrin cavity in these films.

Attempts to determine the coverage electrochemically were unsuccessful,[37] presumably due to the complex topography of these cavity-containing films. However, it is believed that the films are homogeneous monolayers, and permeability arises from the packing order of each derivative, rather than from large areas of uncoated gold.

In all of the results, the monothiolated derivatives were found to behave quite differently at the gold surface than the multithiolated compounds synthesized here, and the multithiolated cyclodextrins reported by Chung,[10] Rojas *et al.*,[11] and Maeda *et al.*[12] These differences are believed to arise from two factors. The first is the lateral diffusion possible for the monothiolated compounds,[38] but impeded considerably for the multithiolated molecules. The other factor is the freedom experienced by the cyclodextrin torus of the monothiolated compounds to orient in a way favorable to intermolecular interactions. The multithiolated molecules are basically restricted to an orientation with the torus C_n axis perpendicular to the gold surface, once a second thiol group is bound to the gold surface.

From these data a model for the organization of the cyclodextrin derivatives in the chemisorbed films has been developed and is depicted in Figure 8. In this model, the cyclodextrin tori are located as an outermost layer on top of the spacers for all derivatives, and the spacers are oriented perpendicular to the surface. This is in contrast to being tilted from the normal as is seen for alkanethiols.[39] The tilt angles observed in films of the latter are attributed to interactions between the closely packed alkyl chains, which are presumably absent in the case of the cyclodextrin derivatives, because of the large interchain distance imposed by the bulky cyclodextrin heads. The spacers in the monothiolated derivatives give more mobility to the cyclodextrin tori to align themselves in the top layer, optimizing intermolecular hydrogen bonding, in contrast to the multi-

(37) Underpotential deposition with $CuSO_4$ and gold oxidation produced unsatisfactory results for coverage determination.

(38) See ref 33, p 296.

(39) Nuzzo, R. G.; Fusco, F. A.; Allara, D. L. *J. Am. Chem. Soc.* **1987**, *109*, 2358.

thiolated derivatives, in which the cyclodextrin tori C_n axes are held perpendicular to the surface normal. The packing density of the tilted cyclodextrin tori increases with increased spacer length. A similar model has also been proposed for metalloporphyrins with either one or two thiol groups, although a tilt angle of the monothiolated metalloporphyrins is postulated.[40]

Conclusions

Several mono- and multithiolated cyclodextrin derivatives with different spacer groups have been synthesized and purified. These cyclodextrins adsorb on gold surfaces, forming films of different thicknesses and packing densities. In all cases the cyclodextrin cavities form the outermost layer of the system, and it is possible to control the orientation of the cyclodextrin cavity in these films by varying the number of thiol anchors and the length of spacer between the cavity and thiol group.

A primary goal in future work is the use of the cyclodextrin cavity in the formation of surface-bound-host−guest inclusion compounds, and thus this orientational control is a crucial advantage of this system, as more or less favorable orientations may be chosen to facilitate or hinder inclusion of the guest molecule, or to control the orientation of the guest molecule in the cavity. In addition to the techniques already described here, atomic force microscopy (AFM) investigations are underway and are expected to provide information not only on the ring orientation but also on the location of the guest molecules in the cavity.

Acknowledgment. The authors would like to thank Professors W. Knoll and G. Wegner for stimulating discussions. The grazing angle FTIR measurements by D.-W. Scholdei are also gratefully acknowledged. Financial support came from Boehringer Mannheim GmbH and the Bundesministerium für Bildung, Forschung und Technologie (Project No. BE022/0319055A).

Supporting Information Available: Text describing more experimental details, in particular synthetic procedures and compound purification and characterization (9 pages). This material is contained in many libraries on microfiche, immediately follows this article in the microfilm version of the journal, can be ordered from the ACS, and can be downloaded from the Internet; see any current masthead page for ordering information and Internet access instructions.

JA9539812

(40) Zak, J.; Yuan, H.; Ho, M.; Woo, L. K.; Porter, M. D. *Langmuir* **1993**, *9*, 2772.